

Studies on the Mechanism of Action of Dextrin–Phospholipase A₂ and Its Suitability for Use in Combination Therapy

Elaine L. Ferguson,^{*,†} Simon C. W. Richardson,[‡] and Ruth Duncan^{*}

Centre for Polymer Therapeutics, Welsh School of Pharmacy, Cardiff University, King Edward VII Avenue, Cardiff, CF10 3XF, U.K.

Received September 15, 2009; Revised Manuscript Received February 15, 2010; Accepted February 17, 2010

Abstract: The bioresponsive conjugate dextrin–phospholipase A₂ (PLA₂) is a novel anticancer polymer therapeutic. Dextrin conjugation decreases PLA₂ bioactivity, but this can be restored following triggered degradation by α -amylase. The conjugate displays reduced hemolytic activity but retains, or shows enhanced, cytotoxicity *in vitro* that partially correlates with epidermal growth factor receptor (EGFR) expression. Here, we investigate further the mechanism of action of dextrin–PLA₂ with the aim of judging its potential for combination with tyrosine kinase inhibitors (TKI) and/or chemotherapy and selecting the first models for *in vivo* evaluation. The endocytic fate of Oregon Green (OG)-labeled probes was assessed in MCF-7 cells. Whereas PLA₂-OG showed greatest membrane binding, the dextrin–PLA₂-OG conjugate displayed higher internalization. Moreover, cells incubated with PLA₂-OG and dextrin–PLA₂-OG showed an altered pattern of intracellular vesicle distribution compared to dextrin–OG. When cell lines known to express different levels of EGFR were used to assess cytotoxicity, free PLA₂ activity was enhanced by addition of EGF whereas the conjugate was less cytotoxic, perhaps due to differences in their PK/PD profile. Co-incubation of cells with the TKI inhibitor, gefitinib, led to reduced cytotoxicity of both PLA₂ and dextrin–PLA₂ suggesting a TK-mediated PLA₂ mechanism of action. However, the enhanced cytotoxicity seen in the presence of doxorubicin suggested potential for development of a dextrin–PLA₂/doxorubicin combination therapy.

Keywords: Polymer therapeutics; cancer; PLA₂; dextrin; anticancer conjugates; nanomedicines; PUMPT

Introduction

Earlier diagnosis and the development of improved therapeutics are contributing to reduced mortality for many cancers.¹ Nevertheless prognosis is still poor for those

patients affected by metastatic disease. Better treatments are beginning to arise from both the development of “molecular-target specific” anticancer agents² and design of innovative drug delivery systems, including first generation nanomedicines.^{3–5} In this context the rationale for design, and current clinical status of anticancer polymer therapeutics,

* Corresponding authors. E.L.F.: mailing address, Wound Biology Group, Tissue Engineering & Reporative Dentistry, School of Dentistry, Cardiff University, Heath Park, Cardiff, CF14 4XY, U.K.; tel, 029 20745454; fax, 029 20742442; e-mail, FergusonEL@cf.ac.uk. R.D.: e-mail, profruthduncan@btinternet.com.

† Current address: Wound Biology Group, Tissue Engineering & Reporative Dentistry, School of Dentistry, Cardiff University, Heath Park, Cardiff, CF14 4XY, U.K.

‡ Current address: Department of Pharmaceutical, Chemical and Environmental Science, Grenville Building, University of Greenwich Medway Campus, Chatham Maritime, Kent, ME4 4TB, U.K.

- (1) Jemal, A.; Tiwari, R. C.; Murray, T.; Ghafoor, A.; Samuels, A.; Ward, E.; Feuer, E. J.; Thun, M. J. Cancer statistics, 2005. *CA Cancer J. Clin.* **2004**, *54*, 8–29.
- (2) Lapenna, S.; Giordano, A. Cell cycle kinases as therapeutic targets for cancer. *Nat. Rev. Drug Discovery* **2009**, *8*, 547–566.
- (3) Duncan, R. Polymer conjugates as anticancer nanomedicines. *Nat. Rev. Cancer* **2006**, *6*, 688–701.
- (4) Lammers, T.; Hennink, W. E.; Storm, G. Tumour-targeted nanomedicines: principles and practice. *Br. J. Cancer* **2008**, *99*, 392–397.
- (5) Ferrari, M. Cancer nanotechnology: opportunities and challenges. *Nat. Rev. Cancer* **2005**, *5*, 161–171.

including polymer–protein and polymer–drug conjugates, has recently been reviewed.^{6,7} Moreover, the growing understanding of the pathophysiological and molecular basis of cancer is bringing a sound rationale for novel multimodal combinations.⁸ The most exciting new polymer conjugates are those directed against emerging molecular targets,⁹ and those designed to deliver combination therapy.^{10–12}

Altered lipid biosynthesis and deregulated lipogenesis are typical features of cancer. Consequently, these pathways are being investigated as novel therapeutic targets¹³ and lipolytic phospholipase A₂ (PLA₂) enzymes¹⁴ are being explored as novel anticancer agents. Although crotoxin, a PLA₂ from snake venom (*Crotalus durissus terrificus*), has recently shown activity in phase I clinical trials against breast, bladder, cervix and lung cancer,¹⁵ significant nonspecific toxicity was also seen, thus limiting potential for further development. Thus, with the aim of reducing PLA₂ toxicity and enhancing tumor targeting by the EPR-mediated effect,^{3,4} we synthesized a dextrin–PLA₂ conjugate¹⁶ that exemplifies the novel concept termed “polymer masked-unmasked protein therapy”

(PUMPT).^{17,18} PUMPT uses a biodegradable polymer to transiently mask the bioactivity (including toxicity) of the protein or peptide to which it is bound, and thus can enhance stability and/or diminish toxicity in transit.¹⁷ On arrival at the target site triggered degradation of the polymer is used to regenerate bioactivity with time.^{17,18} Dextrin (α -1,4 polyglucose) was chosen for conjugation as it is degraded by α -amylase, an enzyme present in all extracellular fluids, but moreover it shows elevated levels (up to 85-fold) in some tumors.¹⁹ Previous studies showed that α -amylase triggered degradation was able to fully regenerate dextrin–PLA₂ bioactivity¹⁶ and that the conjugate displayed retained or enhanced cytotoxicity *in vitro*. Unlike PLA₂ it was not hemolytic showing the potential of conjugation to diminish nonspecific toxicity.¹⁶

Although PLA₂ biochemistry is well documented,^{14,20,21} its mechanism of tumor cell cytotoxicity is still the subject of much debate. Several studies have shown correlation between epidermal growth factor receptor (EGFR) expression and sensitivity to PLA₂.^{22,23} However, both stimulatory and inhibitory effects have been reported, perhaps due to PLA₂ and cell type and/or concentration effects. As EGFR expression is higher in many tumors (e.g., breast, glioma, lung, bladder and colon cancer), and it is often a clinical marker of poor prognosis and poor response to treatment (reviewed in refs 24 and 25), EGFR localization would provide an additional opportunity to impart dextrin–PLA₂ with tumor selectivity. In theory, dextrin–PLA₂ might act by causing membrane damage, localization to EGFR with modulation

- (6) Pasut, G.; Veronese, F. M. PEG conjugates in clinical development or use as anticancer agents: an overview. *Adv. Drug Delivery Rev.* **2009**, *61*, 1177–1188.
- (7) Vicent, M. J.; Ringsdorf, H. Duncan, R. Polymer Therapeutics: Clinical Applications and Challenges for Development. *Adv. Drug Delivery Rev.* **2009**, *61*, 1117–1120.
- (8) Greco, F.; Vicent, M. J. Combination Therapy: Opportunities and Challenges for Polymer-Drug Conjugates as Anticancer Nanomedicines. *Adv. Drug Delivery Rev.* **2009**, *61*, 1203–1213.
- (9) Satchi-Fainaro, R.; Puder, M.; Davies, J. W.; Tran, H. T.; Sampson, D. A.; Greene, A. K.; Corfas, G.; Folkman, J. Targeting angiogenesis with a conjugate of HPMA copolymer and TNP-470. *Nat. Med.* **2004**, *10*, 225–261.
- (10) Vicent, M. J.; Greco, F.; Nicholson, R. I.; Duncan, R. Polymer-drug conjugates as a novel combination therapy for the treatment of hormone-dependent cancers. *Angew. Chem., Int. Ed.* **2005**, *44*, 2–6.
- (11) Lammers, T.; Subr, V.; Ulbrich, K.; Peschke, P.; Huber, P. E.; Hennink, W. E.; Storm, G. Simultaneous delivery of doxorubicin and gemcitabine to tumors in vivo using prototypic polymeric drug carriers. *Biomaterials* **2009**, *30*, 3466–3475.
- (12) Lammers, T.; Subr, V.; Peschke, P.; Kuhnlein, R.; Hennink, W. E.; Ulbrich, K.; Kiessling, F.; Heilmann, M.; Debus, J.; Huber, P. E.; Storm, G. Image-guided and passively tumour-targeted polymeric nanomedicines for radiochemotherapy. *Br. J. Cancer* **2008**, *99*, 900–910.
- (13) Mashima, T.; Seimiya, H.; Tsuruo, T. *De novo* fatty-acid synthesis and related pathways as molecular targets for cancer therapy. *Br. J. Cancer* **2009**, *100*, 1369–1372.
- (14) Cummings, B. S. Phospholipase A₂ as targets for anti-cancer drugs. *Biochem. Pharmacol.* **2007**, *74*, 949–959.
- (15) Cura, J. E.; Blanzaco, D. P.; Brisson, C.; Cura, M. A.; Cabrol, R.; Larrateguy, L.; Mendez, C.; Sechi, J. C.; Silveira, J. S.; Theiller, E.; de Roodt, A. R.; Vidal, J. C. Phase I and pharmacokinetics study of crotoxin (cytotoxic PLA₂, NSC-624244) in patients with advanced cancer. *Clin. Cancer Res.* **2002**, *8*, 1033–1041.
- (16) Ferguson, E. L.; Duncan, R. Dextrin-phospholipase A₂: Synthesis and Evaluation as a Novel Bioresponsive Anticancer Conjugate. *Biomacromolecules* **2009**, *10*, 1358–1364.
- (17) Duncan, R.; Gilbert, H. R. P.; Carbajo, R. J.; Vicent, M. J. Polymer Masked-Unmasked Protein Therapy (PUMPT) 1. Bioresponsive dextrin-trypsin and -MSH conjugates designed for α -amylase activation. *Biomacromolecules* **2008**, *9*, 1146–1154.
- (18) Hardwicke, J.; Ferguson, E. L.; Moseley, R.; Stephens, P.; Thomas, D.; Duncan, R. Dextrin-rhEGF conjugates as bioresponsive nanomedicines for wound repair. *J. Controlled Release* **2008**, *130*, 275–283.
- (19) Inaji, H.; Koyama, H.; Higashiyama, M.; Noguchi, S.; Yamamoto, H.; Ishikawa, O.; Omichi, K.; Iwanaga, T.; Wada, A. Immunohistochemical, ultrastructural and biochemical studies of an amylase-producing breast carcinoma. *Virchows Arch. A: Pathol. Anat. Histopathol.* **1991**, *419*, 29–33.
- (20) Scott, D. L.; White, S. P.; Otwinowski, Z.; Yuan, W.; Gelb, M. H.; Sigler, P. B. Interfacial catalysis: the mechanism of phospholipase A₂. *Science* **1990**, *250*, 1541–1546.
- (21) van den Berg, B.; Tessari, M.; Boelens, R.; Dijkman, R.; de Haas, G. H.; Kaptein, R.; Verheij, H. M. NMR structures of phospholipase A₂ reveal conformational changes during interfacial activation. *Nat. Struct. Biol.* **1995**, *2*, 402–406.
- (22) Donato, N. J.; Martin, C. A.; Perez, M.; Newman, R. A.; Vidal, J. C.; Etcheverry, M. Regulation of epidermal growth factor receptor activity by crotoxin, a snake venom phospholipase A₂ toxin. A novel growth inhibitory mechanism. *Biochem. Pharmacol.* **1996**, *51*, 1535–1543.
- (23) Zhao, S.; Du, X. Y.; Chen, J. S.; Zhou, Y. C.; Song, J. G. Secretory phospholipase A₂ inhibits epidermal growth factor-induced receptor activation. *Exp. Cell Res.* **2002**, *279*, 354–364.
- (24) Baselga, J.; Arteaga, C. L. Critical update and emerging trends in epidermal growth factor receptor targeting in cancer. *J. Clin. Oncol.* **2005**, *23*, 2445–2459.

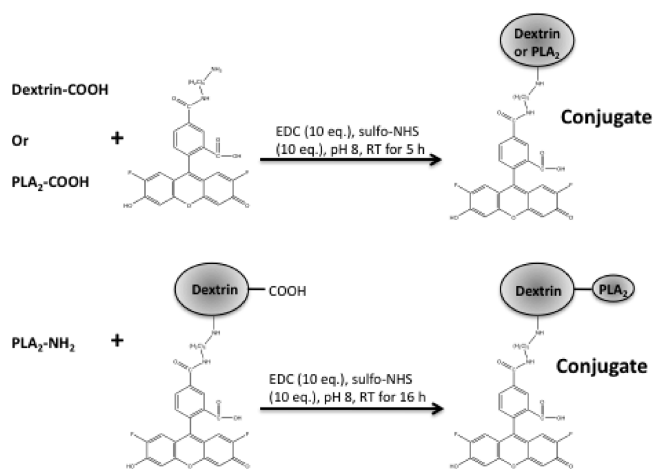
of EGFR-related signal transduction and/or following endocytic uptake by causing damage to endosomal or lysosomal membranes. Therefore, the aim of this study was to investigate further the mechanism(s) of action of dextrin-PLA₂, in particular to define its endocytosis and trafficking pathways using MCF7 cells, to elucidate dextrin-PLA₂ cytotoxicity in tumor cells having a different degree of EGFR expression and to conduct preliminary experiments that might guide future use in combination regimes. Oregon Green (OG)-labeled dextrin, PLA₂ and dextrin-PLA₂ conjugates were synthesized to monitor cellular uptake and intracellular fate. Cytotoxicity was assessed using the MTT assay in cell lines that display different levels of EGFR expression; B16F10 (no human receptors/cell), MCF-7 (8×10^2 /cell),²⁶ HT29 (4.4×10^4 /cell).²⁷ Finally to understand better opportunities for combination therapy, dextrin-PLA₂ cytotoxicity was assessed in MCF-7 cells coincubated with EGF, the tyrosine kinase inhibitor (TKI) gefitinib or doxorubicin. Both are commonly used in combination chemotherapy regimes.

Experimental Section

Materials and Cells. Type 1 dextrin from corn ($M_w \sim 50,000$ g/mol) was from ML laboratories (Keele, U.K.) and gefitinib a kind gift from AstraZeneca (Macclesfield, U.K.). Dextrin-PLA₂ conjugates were synthesized and characterized as previously described.¹⁶ EGF was from Prospec-Tany Technogene Ltd. (Rehovot, Israel). PLA₂ from honeybee venom, 1-ethyl-3-(3-dimethylaminopropyl carbodiimide hydrochloride) (EDC), sodium hydroxide, tissue culture grade dimethyl sulfoxide (DMSO), 3-(4,5-dimethylthiazol-2-yl)-2,5-diphenyl tetrazolium bromide (MTT) and optical grade DMSO were all from Sigma-Aldrich (Poole, U.K.). *N*-Hydroxysulfosuccinimide (sulfo-NHS) was from Fluka (Gillingham, U.K.). Oregon Green 488 cadaverine *5-isomer (OG) was from Invitrogen Molecular Probes (Paisley, U.K.). Unless otherwise stated, all chemicals were of analytical grade. All solvents were of general reagent grade (unless stated) and were from Fisher Scientific (Loughborough, U.K.).

The MCF-7 human breast carcinoma cell line was kindly provided by Tenovus Centre for Cancer Research (Cardiff University, U.K.). HT29 human colon cancer cells were obtained from the European Collection of Cell Cultures

Table 1. Characteristics of OG-Labeled Conjugates



compound	molar ratio (OG: dextrin or PLA ₂ equiv)	labeling efficiency (μ g OG/mg conjugate)	free OG (% of total)
dextrin-OG	0.51	4.96	0.49
PLA ₂ -OG	0.11	3.37	0.83
dextrin-PLA ₂ -OG	0.34 (OG: dextrin) 1.93 (OG: PLA ₂ equiv)	3.15	1.51

(ECCAC; Wiltshire, U.K.). B16F10 murine melanoma was from the American Type Culture Collection (ATCC; Manassas, VA). All cell lines were confirmed mycoplasma free. Fetal calf serum (FCS), 0.05% w/v trypsin-0.53 mM EDTA and RPMI 1640 with L-glutamine (with and without phenol red as pH indicator) were from Invitrogen Life Technologies (Paisley, U.K.). Monoclonal anti-EEA1 (human), was from BD Bioscience (Oxford, U.K.); monoclonal anti-LAMP-1 (clone H4A3) was from DSHB (Iowa City, IA). Donkey antimouse and antirabbit secondary antibodies labeled with Alexafluor488 were from Invitrogen (Paisley, U.K.), and donkey antimouse and antirabbit secondary antibodies labeled with Cy5 were from Rockland Immunochemicals (Reading, U.K.).

Synthesis and Characterization of OG-Labeled Probes. First, dextrin-OG, PLA₂-OG and dextrin-PLA₂-OG labeled conjugates were synthesized using OG (cadaverine derivative) and methods described previously for dextrin-PLA₂ conjugation¹⁶ (Table 1). Briefly, to prepare dextrin-OG and PLA₂-OG succinoylated dextrin (150 mg) or PLA₂ (5 mg), respectively, was dissolved under stirring in PBS buffer (1 mL, pH 7.4) in a 10 mL round-bottomed flask. To this, EDC (10 molar equiv) was added and allowed to dissolve for 10 min. Next, sulfo-NHS (10 molar equiv) was added and the mixture stirred for 40 min before addition of OG (2 molar equiv) (from a stock solution of 5 mg/mL in ddH₂O stored at -20°C until use). Then NaOH (0.5 M) was added dropwise to raise the pH to 8.0 and the reaction mixture was left stirring in the dark for 5 h, the reaction being monitored by TLC. To prepare the dextrin-PLA₂-OG conjugate, a dextrin-OG intermediate was first prepared,

- (25) Oliveira, S.; van Bergen en Henegouwen, P. M.; Storm, G.; Schiffelers, R. M. Molecular biology of epidermal growth factor receptor inhibition for cancer therapy. *Expert Opin. Biol. Ther.* **2006**, *6*, 605–617.
- (26) Fitzpatrick, S. L.; LaChance, M. P.; Schultz, G. S. Characterization of epidermal growth factor receptor and action on human breast cancer cells in culture. *Cancer Res.* **1984**, *44*, 3442–3447.
- (27) Heimbrook, D. C.; Stirdivant, S. M.; Ahern, J. D.; Balishin, N. L.; Patrick, D. R.; Edwards, G. M.; Defeo-Jones, D.; FitzGerald, D. J.; Pastan, I.; Oliff, A. Transforming growth factor alpha-Pseudomonas exotoxin fusion protein prolongs survival of nude mice bearing tumor xenografts. *Proc. Natl. Acad. Sci. U.S.A.* **1990**, *87*, 4697–4701.

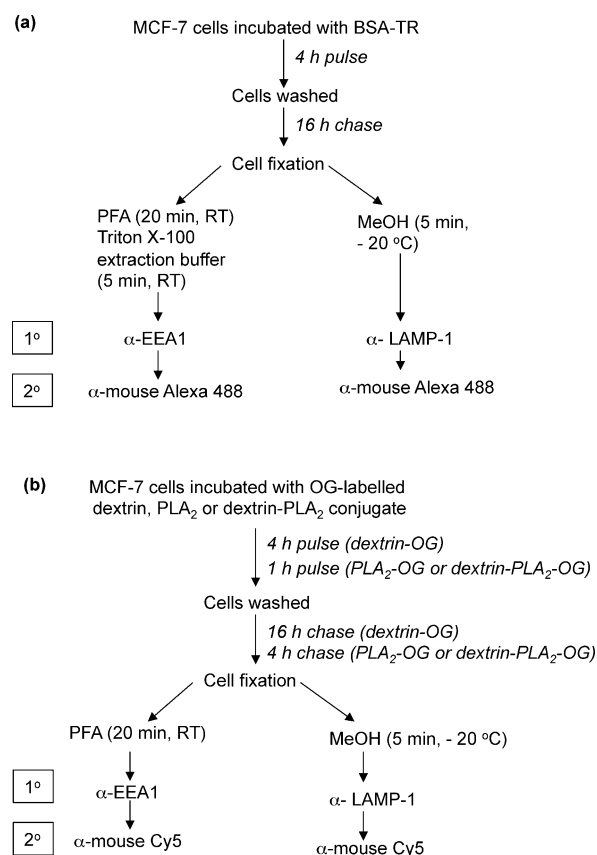
as described above, and then conjugated to unlabeled PLA₂, according to the methods described previously.¹⁶

All the conjugates obtained were purified and characterized by PD-10 column chromatography as described previously.²⁸ The total OG content of each probe was determined spectrophotometrically by measuring absorbance at 485 nm, and the free OG content by measuring fluorescence ($\lambda_{\text{ex}} = 485 \text{ nm}$, $\lambda_{\text{em}} = 520 \text{ nm}$, gain 1000) in the corresponding PD-10 column fractions.¹⁶

Determination of Uptake by Flow Cytometry. To investigate cell association at 37 or 4 °C MCF-7 cells were first seeded in 6-well plates (1×10^6 cells/mL) in WRPMI media supplemented with FCS (5% v/v) and allowed to adhere for 24 h. Experiments at 37 °C were conducted under normal cell culture conditions but for experiments conducted at low temperature the cells were first incubated at 4 °C for 30 min prior to the addition of the probe. Solutions of dextrin-OG, PLA₂-OG or dextrin-PLA₂-OG were freshly prepared in medium equilibrated to either 37 or 4 °C and added to cells at a concentration of 1.5 $\mu\text{g/mL}$ (OG equiv). In both cases, cells were incubated for 1 h and then placed on ice before washing $3 \times$ with ice-cold PBS ($3 \times 1 \text{ mL}$). Then, PBS (1 mL) was added and the cells were harvested into falcon tubes by scraping and centrifuged at 4 °C, 1000g for 5 min. Finally, the cells were resuspended in ice-chilled PBS (200 μL) before analysis using a Becton Dickinson FACSCalibur cytometer equipped with an argon laser (488 nm) and emission filter for 550 nm. Data were collected for 10,000 cell counts per sample and processed using CELLQuest version 3.3 software. MCF-7 cells incubated with medium only were used to account for background fluorescence. Data was acquired in 1024 channels with band-pass filter FL-1 ($530 \text{ nm} \pm 15 \text{ nm}$). Throughout results were expressed as (geometric mean \times % positive cells)/100 and were corrected for cell autofluorescence. Internalization was calculated by subtracting the cell-associated fluorescence at 4 °C (extracellular binding) from that at 37 °C (intracellular uptake plus extracellular binding), and % internalization was derived from the internalized OG-labeled probes compared to the total cell-associated fluorescence (at 37 °C). It is important to note that all uptake studies were undertaken for a maximum of 1 h and at a PLA₂ concentration chosen to ensure no cell toxicity.

Determination of Intracellular Fate by Confocal Microscopy. MCF-7 cells were seeded in 12-well plates containing a sterile glass coverslip in each well (1×10^6 cells/mL) in WRPMI + 5% FCS and allowed to adhere for 24 h. The medium was then replaced with either fresh medium containing dextrin-PLA₂-OG or PLA₂-OG (50 $\mu\text{g/mL}$ OG equiv) and additionally leupeptin (200 μM) to minimize lysosomal proteolytic degradation. The cells were then incubated for 1 h, the medium was removed and the

Scheme 1. Schematic Describing the Protocols Used for Confocal Microscopy Experiments^a



^a Panel a shows the methods used to generate data in Figure 2a, and panel b shows the methods used to generate data in Figures 2b and 2c.

cells were washed with PBS (37 °C, $3 \times 0.5 \text{ mL}$). After the final wash, fresh medium (0.5 mL containing leupeptin (200 μM) was added, and the cells were left for a further 4 h incubation. At the end of this chase period, the medium was removed and the cells were washed with PBS (37 °C, $3 \times 0.5 \text{ mL}$) prior to fixation. Control cells (not incubated with a probe) were used account for autofluorescence.

The methods developed to define the localization of probes to either early endosomes or late endosomes/lysosomes have recently been described,²⁸ and the protocols used here are shown in Scheme 1. Once harvested cells were either fixed in cold methanol (prechilled to -20 °C) and incubated for 5 min at -20 °C or placed in freshly prepared 2% w/v PFA (20 min, at 25 °C). Those cells to be immunolabeled after aldehyde fixation were subjected to detergent extraction with PBS containing 50 mM glycine and 0.2% v/v Triton-X 100 (5 min, 25 °C). Before immunolabeling, nonspecific binding sites were blocked by incubating the cells in 2% v/v goat serum in PBS (60 min, 25 °C). The following dilutions were used for the primary hybridization (60 min at 25 °C): anti-EEA1 (1:300), anti-LAMP-1 (1:10). The secondary hybridization was performed using antimouse antibodies labeled with either Alexafluor 488 or Cy5 for 60 min at 25 °C (1:500).

(28) Richardson, S. C. W.; Wallom, K.-L.; Ferguson, E. L.; Deacon, S. P.; Davies, M. W.; Powell, A. J.; Piper, R. C.; Duncan, R. The use of fluorescence microscopy to define polymer conjugate localisation to late endocytic compartments in fixed and live target cells. *J. Controlled Release* **2008**, *127*, 1–11.

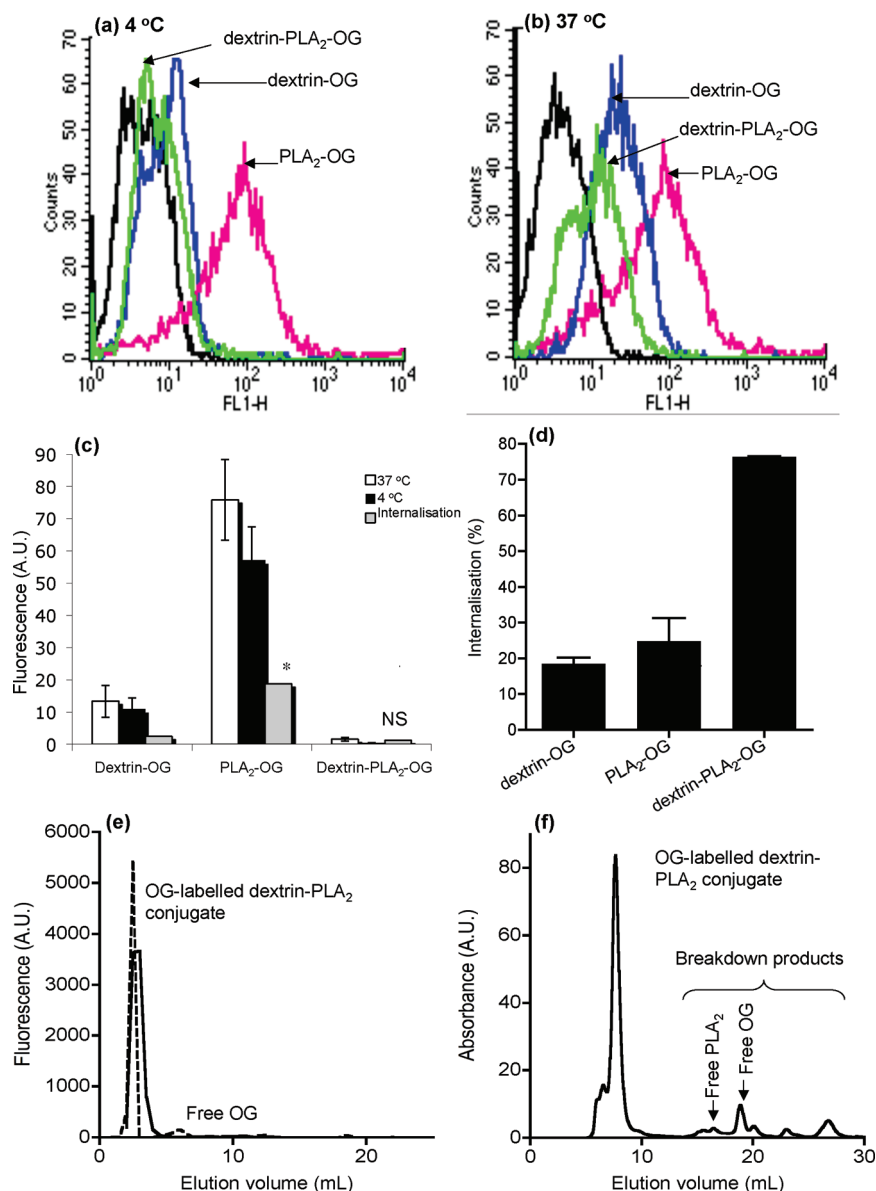


Figure 1. Binding and internalization of OG conjugates by MCF-7 cells and characterization of probes after incubation with cells. Panels a and b show scatter plots for cell-associated fluorescence at 37 and 4 °C (1 h). Panel c shows cell-associated fluorescence for dextrin-OG, PLA₂-OG and dextrin-PLA₂-OG conjugate at 37 and 4 °C. Panel d represents the calculated internalization for each conjugate. Panels e and f show, respectively, PD-10 and FPLC characterization of cell culture medium after the 1 h incubation of the dextrin-PLA₂-OG conjugate with MCF-7 cells, where the solid line represents OG-labeled dextrin-PLA₂ at 0 h and the dashed line represents the OG-labeled conjugate after 1 h incubation in panel e.

Confocal microscopy was performed using a Leica SP5 system. Standard procedures were followed to minimize bleed from one channel to another (giving rise to false positives) and sample photobleaching. All images were collected using monochromatic CCD cameras, and data was collected using dedicated software supplied by the manufacturers. At least three representative images were obtained for each sample and exported as tagged image files (TIF); typical results are shown. Merged images were generated using Photoshop.

Detection of Free OG after Incubation of OG-Labeled Conjugates with Cells. To measure the liberation of free OG in the culture medium or after cell uptake the cell culture medium was subjected to analysis by PD-10 chromatography and/or FPLC.

First, a disposable PD-10 desalting column containing Sephadex G25 was equilibrated with PBS (25 mL added in total). A sample of the culture media was added to the PD-10 column (0.5 mL). Fractions (0.5 mL in PBS) were then collected in 0.5 mL eppendorf tubes (total 45 fractions).

Then, 100 μL of each fraction was placed (in duplicate) into a black 96-well microtiter plate and the fluorescence measured using a fluorescent plate reader ($\lambda_{\text{ex}} = 485 \text{ nm}$, $\lambda_{\text{em}} = 520 \text{ nm}$, gain 1000). The values obtained were then plotted against fraction volume, and free OG content was expressed as percentage of total fluorescence measured in all fractions.

FPLC was used to evaluate the stability of OG-labeled PLA₂ and dextrin-PLA₂ conjugates after incubation with MCF-7 cells (äKTA FPLC; Amersham Pharmacia Biotech, U.K.) using a prepacked Superdex 75 HR/10/30 column with a UV detector and data analysis using Unicorn 3.20 software (Amersham Pharmacia Biotech, U.K.). Cell culture media containing OG-labeled conjugate was removed from the 6-well plate using a pipet and immediately injected (200 μL) into a 100 μL loop using 0.1 M phosphate buffer with 0.15 M sodium chloride, pH 7.4 at 0.5 mL/min as a mobile phase.

Evaluation of Cytotoxicity by MTT Assay. Cytotoxicity was assessed in MCF-7, B16F10, and HT29 cell lines using the MTT assay as previously described²⁹ (72 h incubation). Briefly, cells were seeded into sterile 96-well microtiter plates (MCF-7 and HT29 at 4×10^4 cells/mL; B16F10 at 1×10^4 cells/mL) in 0.1 mL/well of media (WRPMI 1640/McCoy's 5A/RPMI 1640, respectively) containing heat-inactivated FCS (5–10% v/v). They were allowed to adhere for 24 h. The medium was then removed, and filter-sterilized (0.2 μm) test compounds (PLA₂; dextrin or dextrin-PLA₂) were added to the cells to give the final concentrations indicated. After a further 67 h incubation, MTT (20 μL of a 5 mg/mL solution in PBS) was added to each well and the cells were incubated for a further 5 h. The medium was then removed, and the precipitated formazan crystals were solubilized by addition of optical grade DMSO (100 μL). After 30 min absorbance was measured at 550 nm using a microtiter plate reader, and cell viability was expressed as a percentage of the viability of untreated control cells. The IC₅₀ values were expressed as mean \pm SEM.

The effect of EGF on cell proliferation was assessed by measuring viability using the MTT assay (as above) using medium containing heat-inactivated FCS, supplemented with a range of EGF concentrations. An EGF concentration of 10 ng/mL was chosen to study the effect of EGF on PLA₂ and dextrin-PLA₂ mediated cytotoxicity. Again, for these experiments cells were incubated in medium containing heat-inactivated FCS supplemented with EGF and the test compound. Similarly, to study the effect of gefitinib, cells were incubated in complete media including heat-inactivated FCS supplemented with (i) a range of gefitinib concentrations, (ii) gefitinib (1 μM) and various concentrations of PLA₂, or (iii) gefitinib (1 μM) and dextrin-PLA₂. Finally, the effect of doxorubicin alone, or in combination with dextrin-PLA₂ conjugate or PLA₂, was studied. In these

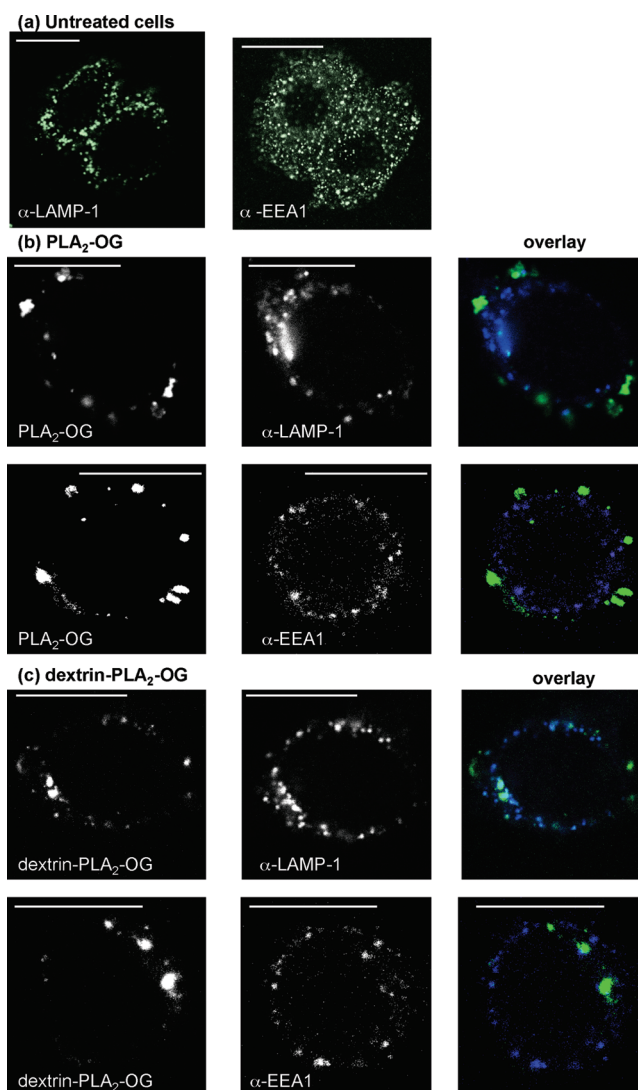


Figure 2. Indirect immunofluorescent confocal micrographs of MCF-7 cells showing cellular localization of PLA₂-OG and dextrin-PLA₂-OG conjugates. Panel a shows distribution of LAMP-1 and EEA1 labeling in untreated MCF-7 cells. Panels b and c show MCF-7 cells after incubation with PLA₂-OG and dextrin-PLA₂-OG, respectively. Cells were incubated with conjugates for 1 h followed by a 4 h chase at 37 °C. Following fixation they were labeled with endosomal (EEA1) and lysosomal (LAMP-1) markers. Fluorescence attributable to the conjugate (line 1), the marker (line 2) and an overlay is shown. Size bar = 10 μm .

experiments PLA₂ or dextrin-PLA₂ was used at a concentration of 50 $\mu\text{g/mL}$ (PLA₂ equiv) and the doxorubicin concentration was varied.

Statistical Analysis. Data are expressed as mean \pm the error, calculated as either standard deviation (SD) where $n = 3$ or standard error of the mean (SEM) where $n > 3$. Statistical significance was set at $p < 0.05$ (indicated by *). Where only two groups were compared, Student's *t* test for a small sample size was used. In situations where more than two groups were compared, evaluation of significance was achieved using a one-way analysis of variance (ANOVA)

(29) Sgouras, D.; Duncan, R. Methods for the evaluation of biocompatibility of soluble synthetic polymers which have potential for biomedical use: 1 — Use of the tetrazolium-based colorimetric assay (MTT) as a preliminary screen for evaluation of in vitro cytotoxicity. *J. Mater. Sci.: Mater. Med.* **1990**, *1*, 61–68.

Table 2. Cytotoxicity of Dextrin–PLA₂ Conjugates in the Presence of EGF or Gefitinib

treatment	IC ₅₀ ^a		
	HT29 ^b	MCF-7 ^b	B16F10 ^c
dextrin	>1000 ^d	>1000 ^d	>1000 ^d
PLA ₂	40.0 ± 2.0	308.6 ± 6.9	108.3 ± 13.8
dextrin–PLA ₂	16.3 ± 2.3	62.9 ± 5.7	133.3 ± 21.1
PLA ₂ + EGF (10 ng/mL)	26.5 ± 4.5	192.5 ± 12.0	194.0 ± 20.8
dextrin–PLA ₂ + EGF (10 ng/mL)	463.6 ± 50.0	91.2 ± 36.7	339.4 ± 70.8
PLA ₂ + gefitinib (1 μM)	254.5 ± 5.2	>500 ^d	>500 ^d
dextrin–PLA ₂ + gefitinib (1 μM)	516.7 ± 12.5	358.3 ± 37.5	383.3 ± 41.7
doxorubicin	na	0.173 ± 0.045	na
doxorubicin + PLA ₂ (50 μg/mL)	na	0.037 ± 0.003	na
doxorubicin + dextrin–PLA ₂ (50 μg/mL)	na	0.008 ± 0.003	na

^a Except for dextrin alone, data expressed in μg/mL (PLA₂ equiv) mean ± SEM; *n* = 18. ^b Cell viability 72 h MTT assay, seeding density 4 × 10⁴ cells/mL for the experiments. ^c Cell viability 72 h MTT assay, seeding density 1 × 10⁴ cells/mL for the experiments. ^d Maximum concentration tested.

followed by Bonferroni *post hoc* tests that correct for multiple comparisons. All statistical calculations were performed using GraphPad Prism, version 4.0c for Macintosh, 2005.

Results

Dextrin–PLA₂ conjugates used in these studies had an average protein content of 6.5 wt % and average molecular weight of 195,000 g/mol. The OG-labeled probes synthesized had labeling efficiencies in the range 3.15–4.96 μg of OG/mg of conjugate, and PD10 column chromatography showed that the conjugates contained <1.51% free OG (Table 1 and Figure 1e for an example).

Uptake and Intracellular Distribution of OG-Labeled Conjugates. Using flow cytometry, all the OG-labeled conjugates showed MCF-7-association after 1 h at 37 °C (Figure 1b,c). However, PLA₂-OG cellular levels were significantly higher than seen for either dextrin–PLA₂-OG or dextrin-OG. In all cases the cell-associated fluorescence was reduced at 4 °C but the PLA₂-OG levels were still highest (Figure 1a,c). Comparison of the extent of internalization showed that the dextrin–PLA₂-OG conjugate displayed greatest uptake at 1 h with 76% of total cell-associated fluorescence being internalized (Figure 1d). PD-10 column chromatography of the incubation medium (for example see Figure 1e) showed a significant increase in free OG levels with incubation for 1 h. For dextrin-OG it rose from 0.49 to 8.41%, for PLA₂-OG from 0.83 to 15.88% and for dextrin–PLA₂-OG from 1.51 to 9.36% free OG. Moreover, FPLC analysis of the culture medium taken after incubation of MCF-7 cells with dextrin–PLA₂-OG revealed additional peaks eluting at times corresponding to free PLA₂, free OG, and additional degradation products (Figure 1f).

Confocal microscopy studies were conducted previously to define the intracellular fate of dextrin-OG in MCF-7 cells and fluorescence labeling was seen in vesicles in the perinuclear region, dextrin-OG fluorescence was exclusively colocalized to both BSA-Texas Red-containing and LAMP-1 positive vesicles,²⁵ i.e. the late endosomes and lysosomes as shown in Figure 2a. Dextrin-OG also showed minimal surface binding,²⁵ consistent with the flow

cytometry results obtained here at 4 °C (Figure 1c). In contrast, in these studies plasma membrane labeling was evident when MCF-7 cells were incubated with both PLA₂-OG and dextrin–PLA₂-OG for 1 h (followed by a 4 h chase in probe free medium at 37 °C). Whereas little intracellular vesicular labeling was seen for PLA₂-OG

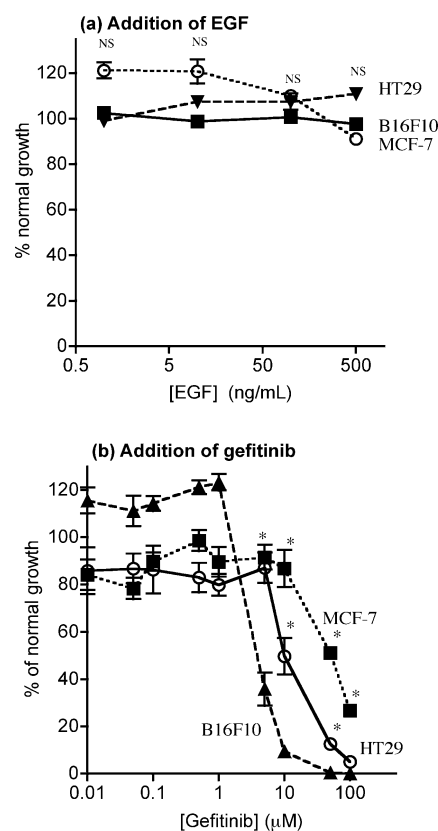


Figure 3. Viability of MCF-7, HT29 and B16F10 cells after incubation (MTT; 72 h) with EGF (panel a) or gefitinib (panel b). Data represent % control cell growth ± SEM (*n* = 18). Where error bars are invisible, they are within the size of data points. NS defines no significant difference, and * indicates significance compared to B16F10 control, *p* < 0.05 (ANOVA and Bonferroni *post hoc* test).

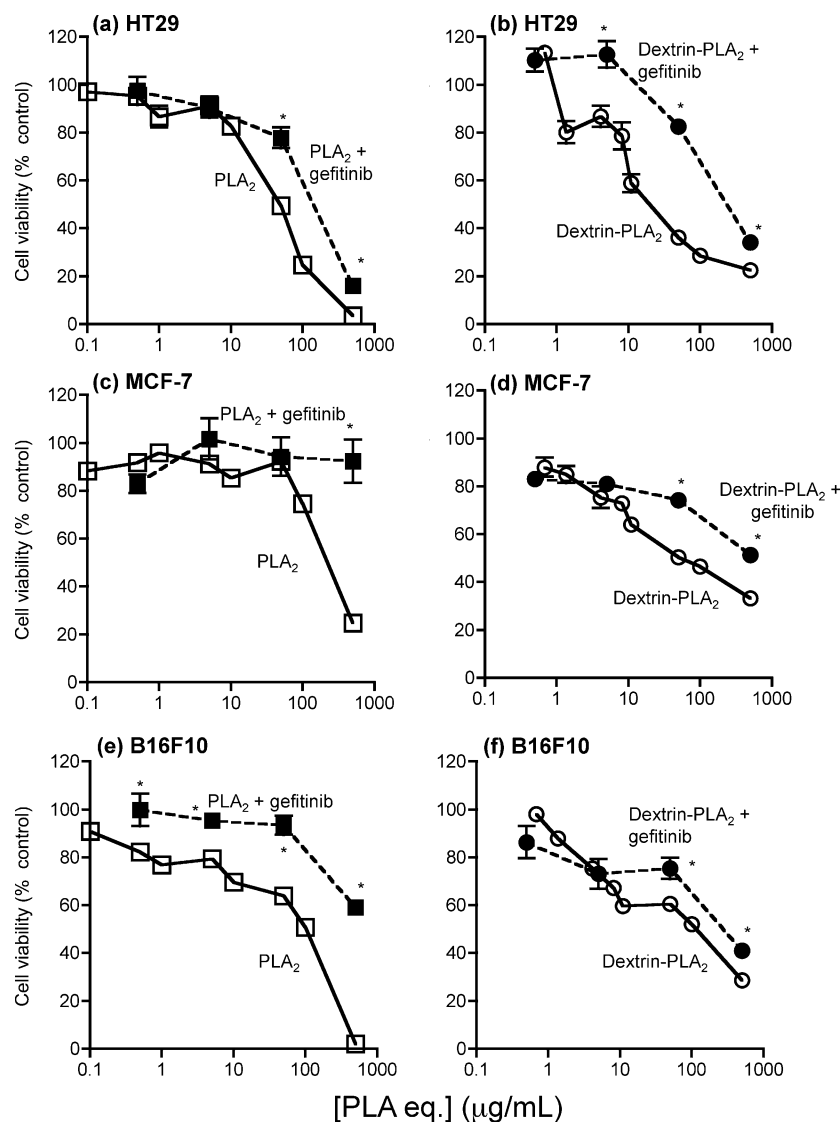


Figure 4. Cytotoxicity (MTT, 72 h) of PLA₂ or dextrin-PLA₂ added in combination with gefitinib (1 μM). Panels a and b show HT29, panels c and d MCF-7 cells and panels e and f B16F10 cells. Data represent mean ± SEM, $n = 18$. * indicates significance $p < 0.05$ compared to PLA₂ or dextrin-PLA₂ control.

(Figure 2b), dextrin-PLA₂-OG was visible in some vesicles (Figure 2c). When indirect immunofluorescence was used to label EEA1 and LAMP-1 positive structures in MCF-7 cells (endosomes and late endosomes/lysosomes respectively), after incubation with PLA₂-OG or dextrin-PLA₂-OG there was a marked change in the intracellular distribution of these vesicles compared to that seen in untreated control cells (Figure 2). Moreover, PLA₂-OG or dextrin-PLA₂-OG fluorescence was seen predominantly around the cell periphery and, in contrast with results obtained for dextrin-OG, there was no colocalization with EEA1 or LAMP-1.

Cytotoxicity of Dextrin-Bound PLA₂ and Its Combinations. All IC₅₀ values obtained for cytotoxicity studies are summarized in Table 2. Dextrin was not toxic toward any of the cell lines up to the 1 mg/mL concentration tested. Free PLA₂ was cytotoxic; HT29 > B16F10 > MCF-7, but dextrin-PLA₂ displayed greater toxicity than

free PLA₂ in HT29 (2.5-fold) and in MCF-7 cells (4.9-fold). For dextrin-PLA₂, cytotoxicity seen was in the order HT29 > MCF-7 > B16F10. As control experiments for the combination studies, cells were incubated with EGF or gefitinib (Figure 3a). Addition of EGF caused no significant change in cell viability, and an EGF concentration of 10 ng/mL was chosen for the combination studies. In contrast, addition of gefitinib caused concentration-dependent toxicity in all cell lines (Figure 3b), and the IC₅₀ values obtained were 2.5 μM (B16F10), 9 μM (HT29) and 55 μM (MCF-7) respectively. For the combination studies it was thus decided to use a nontoxic gefitinib concentration of 1 μM to allow direct comparison of results obtained in different cell lines without the complication of direct gefitinib effects.

Combination of EGF and Dextrin-PLA₂. When cells were incubated with EGF (10 ng/mL), an increase in PLA₂-

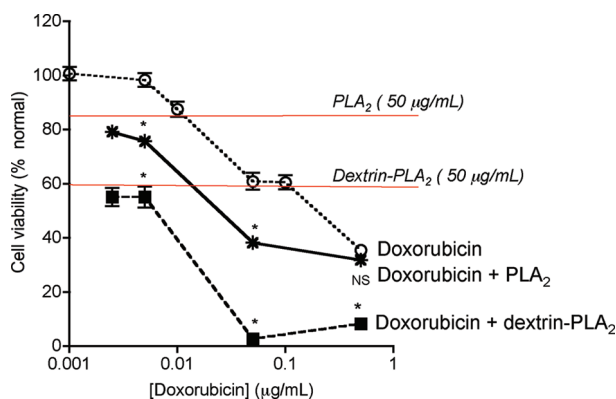


Figure 5. Cell viability (MTT, 72 h) of MCF-7 cells incubated with PLA₂ and dextrin-PLA₂ conjugate (50 μg/mL PLA₂ equiv) in combination with doxorubicin. The toxicity of free doxorubicin and the combinations is shown. The toxicity measured for PLA₂ and dextrin-PLA₂ at the concentration used is illustrated. Data represent mean ± SEM, *n* = 18. * indicates significance *p* < 0.05 compared to doxorubicin control.

mediated toxicity was seen in HT29 and MCF7 cells (~1.5-fold), but there was no effect in B16F10 cells which do not have the hEGF receptor (Table 2). In contrast, when EGF was added together with dextrin-PLA₂, there was a marked decrease in dextrin-PLA₂-mediated toxicity in HT29 cells (30-fold), a smaller decrease in toxicity in B16F10 cells (3-fold) and no significant effect on MCF-7 cells (Table 2). There was a significant difference between the cytotoxicity of the treatment combinations in the different cell types (where *p* < 0.05 (ANOVA and Bonferroni *post hoc* test)).

Combination of Gefitinib and Dextrin-PLA₂. Addition of gefitinib (1 μM) together with PLA₂ and dextrin-PLA₂ led to a decrease in cytotoxicity observed in all cell lines (Figure 4; Table 2) which varied between 1.6- and 6.35-fold reduction for PLA₂ + gefitinib and was a 6- to 32-fold decrease for the dextrin-PLA₂ + gefitinib combination. The effects were most marked for HT29 cells and were least noticeable in B16F10 cells. There was a statistically significant difference between cytotoxicity of the treatment combinations in the different cell types (where *p* < 0.05 (ANOVA and Bonferroni *post hoc* test)).

Combination of Doxorubicin and Dextrin-PLA₂. When incubated with MCF-7 cells, doxorubicin alone was significantly more cytotoxic (IC₅₀ = 173 ng/mL) than either PLA₂ (IC₅₀ = 309 μg/mL) or dextrin-PLA₂ (IC₅₀ = 63 μg/mL). Addition of PLA₂ or dextrin-PLA₂ to increasing concentrations of doxorubicin significantly increased cytotoxicity compared to the doxorubicin control (*p* < 0.05 ANOVA and Bonferroni *post hoc* test) (Figure 5; Table 2). The effect seen was greater than a simple sum of the cytotoxicity of each component.

Discussion

In addition to its presence in venoms (e.g., of snakes and bees), secreted PLA₂ (sPLA₂) is found at high concentrations in human pancreatic secretions, synovial fluid inflammatory

exudates and some tumors. Bee venom sPLA₂ was selected for these studies. All sPLA₂ share a high similarity in their primary structure,³⁰ they hydrolyze the *sn*-2 position of membrane glycerophospholipids to liberate arachidonic acid (AA)¹⁴ and frequently display common inflammatory and analgesic effects. Different subfamilies of sPLA₂ do, however, serve very specific physiological functions in different species. sPLA₂ has been explored as an anticancer agent in its own right,¹⁵ as the active component of nanosized drug delivery systems (e.g., liposomal formulations^{31,32} and PEG conjugates³³), and native human sPLA₂ present in the tumor interstitium³⁴ is being explored as a trigger for degradation of specifically designed “LiPlasomes”. These vesicles can be used to entrap anticancer agents and can also be made from antitumor ether lipids.³⁵ We have proposed dextrin-PLA₂ as a bioresponsive anticancer polymer therapeutic in the context of PUMPT,¹⁶ and/or as a trigger for liposomal permeabilization; i.e. as a new example of polymer-enzyme liposome therapy (PELT).^{36,37} Therefore, prior to designing protocols for *in vivo* studies it was considered important to investigate further the dextrin-PLA₂ mechanism of action, particularly as this could potentially involve multiple cellular targets (Figure 6).

Interfacial catalysis by PLA₂ has been widely studied in terms of enzyme kinetics and EGFR involvement,^{20–24} but its endocytic pathway has not been as well characterized. Most research assumes that PLA₂ acts at the cell surface, but there are a number of factors that suggest

- (30) Davidson, F. F.; Dennis, E. A. Evolutionary relationships and implications for the regulation of phospholipase A₂ from snake venom to human secreted forms. *J. Mol. Evol.* **1990**, *3*, 228–238.
- (31) Freitas, T. V.; Frezard, F. Encapsulation of native crotoxin in liposomes: a safe approach for the production of antivenom and vaccination against *Crotalus durissus terrificus* venom. *Toxicon* **1997**, *35*, 91–100.
- (32) Magalhaes, T.; Viotti, A. P.; Gomes, R. T.; de Freitas, T. V. Effect of membrane composition and of co-encapsulation of immunostimulants in a liposome-entrapped crotoxin. *Biotechnol. Appl. Biochem.* **2001**, *33*, 61–64.
- (33) Bianco, I. D.; Daniele, J. J.; Delgado, C.; Fisher, D.; Francis, G. E.; Fidelio, G. D. Coupling reaction and properties of poly(ethylene glycol)-linked phospholipases A₂. *Biosci., Biotechnol., Biochem.* **2002**, *66*, 722–729.
- (34) Tribler, L.; Jensen, L. T.; Jørgensen, K.; Brünner, N.; Gelb, M. H.; Nielsen, H. J.; Jensen, S. S. Increased expression and activity of group IIA and X secretory phospholipase A₂ in peritumoral versus central colon carcinoma tissue. *Anticancer Res.* **2007**, *27*, 3179–3185.
- (35) Kaasgaard, T.; Andresen, T. L.; Jensen, S. S.; Holte, R. O.; Jensen, L. T.; Jørgensen, K. Liposomes containing alkylated methotrexate analogues for phospholipase A₂ mediated tumor targeted drug delivery. *Chem. Phys. Lipids* **2009**, *157*, 94–103.
- (36) Satchi-Fainaro, R.; Hailu, H.; Davies, J. W.; Summerford, C.; Duncan, R. PDEPT: Polymer directed enzyme prodrug therapy: II. HPMa copolymer-β-lactamase and HPMa copolymer-C-Dox as a model combination. *Bioconjugate Chem.* **2003**, *14*, 797–804.
- (37) Ferguson, E. L.; Duncan, R. Investigating a Dextrin-Phospholipase A₂ Conjugate as a Trigger for Polymer Enzyme Liposome Therapy (PELT). *Proc. Int. Symp. Pol. Ther. (Valencia, Spain)* **2008**, *7*, 96.

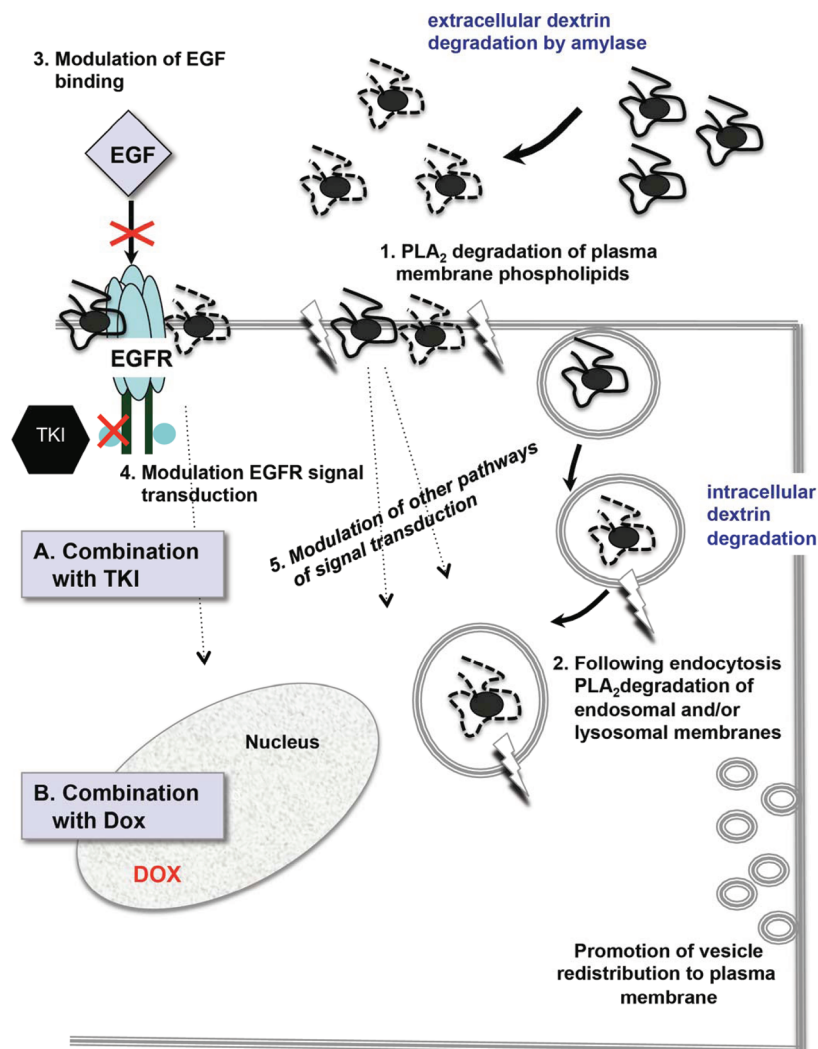


Figure 6. Schematic showing potential mechanisms of dextrin-PLA₂ action.

that PLA₂ could preferentially act on endosomal or other intracellular membranes following endocytosis. These include (i) PLA₂'s preference for curved membranes^{38,39} and (ii) the potentially higher endosomal content of phospholipids that are preferentially hydrolyzed by PLA₂ (phosphatidylcholine (PC), phosphatidylethanolamine (PE) and sphingomyelin (SM)).^{40,41} Quantitative measurements are difficult using fluorescent probes, but as the OG conjugates prepared here had a similar OG loading and purity (Table 1), and the rate of OG liberation during incubation *in vitro* culture was relatively similar (8–16%

OG released/h), it was possible to make meaningful comparisons. Also it should be noted that past studies have shown that such OG probes show minimal pH- and concentration-dependent quenching,⁴² and traces of released OG are readily removed during cell washing and do not significantly affect uptake observations.²⁸ Clearly, PLA₂-OG showed much higher levels of MCF-7 association (even though this protein liberated OG the fastest (by PD-10 chromatography)). High levels of PLA₂ membrane binding were seen at 4 °C (Figure 1c), and this was confirmed using fluorescence microscopy (Figure 2b). These data are consistent with reported bee venom PLA₂ membrane interaction that is mediated by a domain composed mainly of hydrophobic residues and two basic residues promoting interaction with anionic phospholipids

- (38) Grainger, D. W.; Reichert, A.; Ringsdorf, H.; Salesse, C.; Davies, D. E.; Lloyd, J. B. Mixed monolayers of natural and polymeric phospholipids: structural characterization by physical and enzymatic methods. *Biochim. Biophys. Acta* **1990**, *1022*, 146–154.
- (39) Best, K. B.; Ohan, A. J.; Hawes, A. C.; Hazlett, T. L.; Gratton, E.; Judd, A. M.; Bell, J. D. Relationship between erythrocyte membrane phase properties and susceptibility to secretory phospholipase A₂. *Biochemistry* **2002**, *41*, 13982–13988.
- (40) Monteggia, E.; Colombo, I.; Guerra, A.; Berra, B. Phospholipid distribution in murine mammary adenocarcinomas induced by activated neu oncogene. *Cancer Detect. Prev.* **2000**, *24*, 207–211.

- (41) Diez, E.; Chilton, F. H.; Stroup, G.; Mayer, R. J.; Winkler, J. D.; Fonteh, A. N. Fatty acid and phospholipid selectivity of different phospholipase A₂ enzymes studied by using a mammalian membrane as substrate. *Biochem. J.* **1994**, *301*, 721–726.
- (42) Seib, F. P.; Jones, A. T.; Duncan, R. Endocytic behaviour of linear, branched PEI and cationic PAMAM dendrimers in B16F10 melanoma cells. *J. Controlled Rel.* **2007**, *17*, 291–300.

such as phosphatidylserine (PS).⁴³ Dextrin-OG and the dextrin-PLA₂-OG conjugates showed lower levels of membrane association, but interestingly the dextrin-PLA₂ conjugate displayed a proportionally much greater degree of internalization (Figure 2d).

Fluorescence microscopy has confirmed that MCF-7 cells endocytose dextrin-OG, and that a 1 h pulse followed by a 4 h chase is sufficient time for dextrin-OG trafficking into the lysosomes.²⁸ In contrast, here microscopy revealed that PLA₂-OG and the dextrin-PLA₂-OG exhibit a distinct pattern of cell-associated fluorescence in MCF-7 cells. In particular, labeled vesicles were visible in the cortical region (Figure 2b,c). Such observations would be consistent with the hypothesis that PLA₂-mediated cell membrane damage causes redirection of intracellular vesicles toward the cell membrane to repair damage,⁴⁴ and/or that PLA₂/dextrin-PLA₂ action occurs, at least in part, within endosomal or lysosomal vesicles causing damage there or altering trafficking. The subtle differences in lipid composition between the cell, endosomal and lysosomal membranes might encourage PLA₂/dextrin-PLA₂ hydrolysis of the vesicular membrane lipids, which in turn could result in cell death by the release of acidic contents and/or lysosomal enzymes. Moreover, it has been shown that crotoxin induces upregulation of lysosomal enzymes, and an increased formation of autophagosomes and autophagic vacuoles.⁴⁵

A number of studies have shown a correlation between EGFR expression and cell sensitivity to PLA₂.^{22,23} Zhao et al.²³ reported inhibition of EGF-induced receptor activation by PLA₂ from *Agkistrodon halys pallas* in A431 (human epithelial carcinoma) cells, leading to a rise in intracellular ceramide and the release of AA. They therefore suggested that PLA₂ downregulates EGFR-mediated intracellular signal transduction. Conversely, Donato et al.²² noted a crotoxin-mediated activation of EGFR in a number of squamous carcinoma cell lines and found that the EGFR-dependent sensitivity to the cytotoxic effects of PLA₂ was altered when they were coincubated with a combination of EGF and PLA₂. Those cells expressing the highest levels of EGFR were the most sensitive to PLA₂, although direct binding of crotoxin to EGFR was not observed. The different outcomes of these studies were attributed to the different PLA₂ types used, since there remains a threshold level of identity of about 30% between any PLA₂ from the same group. Here, PLA₂ response to addition of EGF (10 ng/mL) varied for PLA₂

and dextrin-PLA₂ and also the cell line studied. This may be due to the fact that activation of EGFR induces upregulation of EGFR⁴⁶ which might promote PLA₂ activity following EGFR colocalization. However, over time subsequent endocytosis of EGFR-ligand complexes by clathrin-coated pits leads to lysosomal degradation resulting in subsequent EGFR downregulation and an associated reduction of signaling.⁴⁷ As “unmasking” of the dextrin-PLA₂ conjugate takes time, it is unlikely that these kinetics would be favorable for its EGF promotion of activity.

The TKI, gefitinib (also known as ZD1839 or Iressa), competes for the intracellular catalytic site of EGFR, and in so doing inhibits receptor activation by blocking downstream signal transduction pathways without affecting EGFR expression. It was considered important to study the dextrin-PLA₂/gefitinib combination (i) to investigate whether TK activity was important for PLA₂ activity and (ii) to define the potential clinical impact of using this combination of drugs. Addition of gefitinib (1 μ M) led to diminished cytotoxicity of PLA₂ and dextrin-PLA₂ in all cell lines (Figure 4, Table 2). These observations were consistent with previous studies that have shown that PLA₂ requires EGFR TK activity for cytotoxicity⁴⁸ and that crotoxin stimulates EGFR TK phosphorylation in A431 cells *in vitro*.²² EGF triggers membrane ruffling and macropinocytosis in epidermoid cells,^{49,50} and since there is evidence that TK activity is required for this process, addition of gefitinib may indirectly lead to membrane destabilization and/or alterations in endocytosis that would also influence dextrin-PLA₂-related toxicity. Whatever the precise mechanism, the EGFR TK is implicated in dextrin-PLA₂ cytotoxicity and it appears that it would be sensible to avoid dextrin-PLA₂ combination with a TKI. Moreover, the recent clinical trial failure of the TKIs, gefitinib and erlotinib, in a combination with chemotherapy in pretreated non small cell lung cancer (NSCLC) patients has illustrated the need for greater consideration of potential combinations at an early stage.⁵¹

- (43) Bollinger, J. G.; Diraviyam, K.; Ghomashchi, F.; Murray, D.; Gelb, M. H. Interfacial binding of bee venom secreted phospholipase A₂ to membranes occurs predominantly by a nonelectrostatic mechanism. *Biochemistry* **2004**, *43*, 13293–13304.
- (44) Reddy, A.; Caler, E. V.; Andrews, N. W. Plasma membrane repair is mediated by Ca²⁺-regulated exocytosis of lysosomes. *Cell* **2001**, *106*, 157–169.
- (45) Yan, C. H.; Liang, Z. Q.; Gu, Z. L.; Yang, Y. P.; Reid, P.; Qin, Z. H. Contributions of autophagic and apoptotic mechanisms to CrTX-induced death of K562 cells. *Toxicon* **2006**, *47*, 521–530.

- (46) Mathur, R. S.; Mathur, S. P.; Young, R. C. Up-regulation of epidermal growth factor-receptors (EGF-R) by nicotine in cervical cancer cell lines: this effect may be mediated by EGF. *Am. J. Reprod. Immunol.* **2000**, *44*, 114–120.
- (47) Sorkina, T.; Huang, F.; Beguinot, L.; Sorkin, A. Effect of tyrosine kinase inhibitors on clathrin-coated pit recruitment and internalization of epidermal growth factor receptor. *J. Biol. Chem.* **2002**, *277*, 27433–27441.
- (48) Goldberg, H. J.; Viegas, M. M.; Margolis, B. L.; Schlessinger, J.; Skorecki, K. L. The tyrosine kinase activity of the epidermal-growth-factor receptor is necessary for phospholipase A₂ activation. *Biochem. J.* **1990**, *267*, 461–465.
- (49) Araki, N.; Egami, Y.; Watanabe, Y.; Hatae, T. Phosphoinositide metabolism during membrane ruffling and macropinosome formation in EGF-stimulated A431 cells. *Exp. Cell Res.* **2007**, *313*, 1496–1507.
- (50) Hewlett, L. J.; Prescott, A. R.; Watts, C. The coated pit and macropinocytic pathways serve distinct endosome populations. *J. Cell Biol.* **1994**, *124*, 689–703.
- (51) Milano, G.; Spano, J.-P.; Leyland-Jones, B. EGFR-targeting drugs in combination with cytotoxic agents: from bench to bedside, a contrasted reality. *Br. J. Cancer* **2008**, *99*, 1–5.

Observation that doxorubicin cytotoxicity (Figure 5) was enhanced in the presence of PLA₂ and the dextrin-PLA₂ conjugate, and indeed the effect was most pronounced for the conjugate, could provide an important opportunity for combination therapy. Since the dextrin-PLA₂ conjugate alone was inherently more toxic than free PLA₂ in MCF-7 cells, further experiments are needed to define the exact mechanisms responsible. Doxorubicin is still widely used in many of the drug combination regimes used to treat a variety of different tumors, nevertheless its use can be limited by cumulative dose-related cardiotoxicity and the induction of resistance mechanisms. As we have already shown that a polymer conjugate containing both doxorubicin and an aromatase inhibitor displays remarkably enhanced activity,⁷ and there is growing preclinical and clinical evidence to support combination of polymer therapeutics with chemotherapy, endocrine therapy and radiotherapy, there is an urgent need to define dextrin-PLA₂ activity *in vivo* in tumor models having a high/low EGFR receptor status and also using combination chemotherapy protocols. These experiments are critical to see whether clinical evaluation of this approach is justified. Parallel studies to better define dextrin-PLA₂ time-dependent whole body and cellular pharmacokinetics together with intracellular fate/metabolism are needed to guide best dosing schedule and move toward an understanding of the pharmacokinetic-pharmacodynamic relationships for this conjugate.

Conclusions

Dextrin-PLA₂ is a novel biodegradable polymer therapeutic with advantages compared to PEG-PLA₂. Dextrin has the ability to mask and then regenerate full bioactivity of PLA₂ in the presence of amylase, and moreover, use of this biodegradable polymer (whose molecular weight can be tailored to ensure an optimal *in vivo* pharmacokinetic profile) allows repeated dosing without fear of progressive accumulation as might be the case if using a high molecular weight PEG. Dextrin-PLA₂ cytotoxicity correlates in part with EGFR status and, as EGFR-related TK activity is important for cytotoxicity, combination with a TKI such as gefitinib would not be clinically useful. Preliminary experiments show that the conjugate is internalized by endocytosis more readily than PLA₂ alone. The resulting redistribution of intracellular vesicles seen suggests a multimodal mechanism of action involving both plasma- and intracellular-vesicle membrane interactions (Figure 6). Moreover, as dextrin-PLA₂ activity was enhanced by combination with doxorubicin *in vivo* definition of antitumor activity is warranted.

Acknowledgment. E.L.F. would like to thank the Welsh School of Pharmacy and the Centre for Polymer Therapeutics for funding her PhD studies, and we would like to acknowledge support from EPSRC Platform Grant No. EP/C 013220/1.

MP900232A